International Journal of Geosynthetics and Ground Engineering (2023) 9:36
https://doi.org/10.1007/s40891-023-00455-w

TECHNICAL NOTE

Evaluation of Different Protection Systems to Control the Geomembrane Deformations in Liner Applications

Gabriel Orquizas Mattielo Pedroso[1] · **Jefferson Lins da Silva**[2]

Received: 16 March 2023 / Accepted: 8 June 2023

Abstract
In landfill backfill systems and mining tailings piles, it is required to use a protective layer above the geomembrane to prevent physical damage from the overlying granular drainage layer. In this work, an experimental study was carried out to evaluate the deformed surface of a 2-mm-thick HDPE geomembrane from a coarse drainage gravel overlying when placed above a clayed underliner subjected to loads of 600 kPa and 1800 kPa over 100 h. Four nonwoven PP-type geotextiles with a mass per unit area ranging from 550 to 1300 g/m^2 and a layer of 100 mm of clay placed above the geomembrane were tested as protection layers. A machine of reading by coordinates with a grid of 1 mm was used to develop a contour map and the strains were calculated for the whole geomembrane deformed surface in percentage. The results showed that the geomembrane presented puncture and large tensile strain values without protection. The clayed soil was the only protection limiting the tensile strains below the proposed limits. It was verified that at high pressure, the geotextile protection could not avoid a puncture, and although the double nonwoven geotextile reduced the strain values, the GMB area exhibiting strain above the proposed limit was too high and could lead to long-term failure. Even with a lower applied load, the single geotextile protection had 30% of the geomembrane area exceeding the 3% strain threshold. On the other hand, the double geotextile showed a performance improvement presenting 14% of the area exceeding the proposed limit.

Keywords Geomembrane · Protection layer · Strain · Stress crack · Puncture

Introduction

Geomembrane (GMB) has been used as a vital component of a barrier system from leakage for landfill, heap leach, and other applications to minimize the contaminant migration to groundwater [1]. Usually, the barrier system consists of a compacted clay liner or a geosynthetic clay liner in combination with the GMB and a drainage collection layer of coarse material above the composite liner. A large stone aggregate is required for the drainage layer to prevent system clogging [2]. This system provides an excellent barrier with low permeability. However, due to the coarseness of the drainage layer and the overburden stresses from the overlying material on top of it, the GMB can experience significant tensile strains that could lead to leakage throughout the material [3]. Thus, to maintain the integrity of the system, it is desirable the selection of a proper protection layer above the GMB.

A puncture on the GMB is mainly from two mechanisms: short-term punctures and long-term high strains [4]. Short-term puncture is a ductile failure due to construction damage or protruding objects in contact with the GMB [5–7]. Long-term high strain values in the GMB due to the operation load result in brittle failure caused by stress cracking [8, 9].

A nonwoven geotextile above the geomembrane is usually used for preventing short-term puncture from the overlying gravel [1]. To identify the mechanisms and efficiency of nonwoven geotextile protection, Brachman and Sabir [10] defined two effects that lead to this protection: 1- cushioning, which spreads the force of a gravel contact over a larger area, resulting in smaller indentations; 2- membrane tension,

✉ Gabriel Orquizas Mattielo Pedroso
gabriel.pedroso@unesp.br

Jefferson Lins da Silva
jefferson@sc.usp.br

[1] Guaratinguetá Faculty of Engineering, São Paulo State University (UNESP), Av. Dr. Ariberto Pereira da Cunha, n° 333, Portal das Colinas, Guaratinguetá, SP 12.516-410, Brazil

[2] São Carlos School of Engineering, University of São Paulo (USP), Avenida Trabalhador São-carlense, n° 400, Pq Arnold Schimidt, São Carlos, SP 13.566-590, Brazil

Published online: 17 June 2023

which is mobilized when the geotextile deforms. The cylinder test can evaluate the tensile strain and puncture of the geomembrane, and it is a large-scale apparatus that places a liner underneath the GMB, a granular drainage stone above the GMB, and a protection layer between these layers and is subjected to design vertically applied load [8].

Different methodologies for calculating the tensile strain of the GMB were developed to analyze the proper selection of a protection layer. Tognon et al. [8] developed a method applied to deformations selected manually in a single line, considering the vertical displacement and the bending membrane. Hornsey and Wishaw [11] proposed a method considering only the vertical displacement to evaluate the grid scanning of the entire surface of the GMB, removing bias from the operator. Eldesouky and Brachman [12, 13] developed a method that takes into account the GMB strain from irregularly shaped indentations considering the displacement in radial, vertical, and membrane bending directions. Seeger and Muller [14] indicated that the GMB strain should be less than 3% to avoid premature failure due to stress cracking. A 6–8% strain threshold has been recommended by Peggs et al. [15] for smooth GMB. Rowe and Yu [16] for a 2-mm-thick texture GMB proposed a maximum allowable strain of 3% on the base, 4% on slopes, and 5% on the cover.

Several studies on GMB strains on different test conditions and the efficiency of protection systems have been reported and evaluated for landfill [16–18] and mining applications [19–21]. The effect of increasing time and temperature was observed by Sabir and Brachman [22]. The molding moisture content and plasticity of the compacted material beneath the GMB [23]. The nominal grain size and the grain size distribution of the gravel from the drainage layer [18]. Alternative protection layers using geonet, rubber tire shreds, and sand, demonstrating that the sand layer is the most effective protective layer [24, 25]. For mining applications with severe conditions (high stress), Rowe et al. [26] focused on the effect of different underliners, showing that the presence of gravel, the deformability, and the shape of the grading curve affected the maximum tensile strain in the GMB.

Strain area distribution (SAD) curves were developed and used by Hornsey and Wishaw [11], and Marcotte and Fleming [23] as a tool of comparing performance between protection layers. The strain measure method consists of a uniform grid scanning of the geomembrane surface, and the maximum strain is calculated for each grid point. Then, the geomembrane strain is represented on a percentage of the total area above a given strain limit instead of the maximum strain from a manual selection of dimples, however, as most previous studies asses the maximum strain [18, 24–26]. There is limited information about the effectiveness of different protection layers in reducing the tensile strains when considering the cumulative percentage of the total area greater than a threshold strain (SAD curves) and the geomembrane surface strain contours map.

The objective of this study is to evaluate and compare the effectiveness of alternate protection layers taking into consideration the SAD curves and the strain contours map using Hornsey and Wishaw's method for one specific clay foundation, GMB, and coarse gravel overlying. A clayed soil and four nonwoven needle geotextiles were examined to assess the protection layer at two different applied pressures.

Materials and Methods

Underliner Material and Overliner Material

A local native typical underliner material from Brazil was utilized in this paper (Fig. 1a). A silty clay soil with 50%

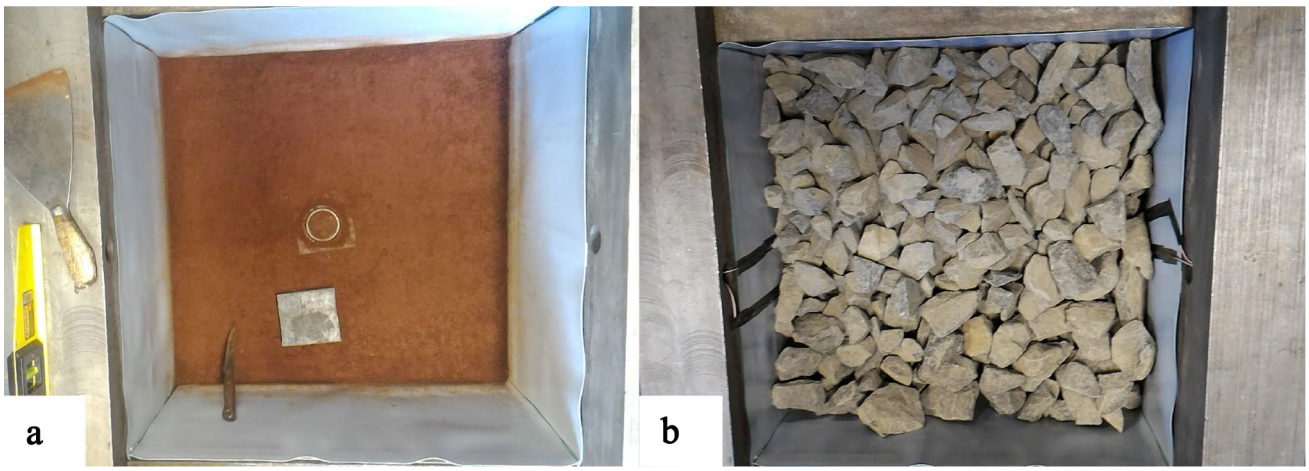

Fig. 1 Photograph of **a** underliner material and **b** overliner material

fines, plastic index of 23, 35–40% low plasticity fines, and maximum particle size of 2 mm (Fig. 2). This clay soil is typically used for CCL construction at state of São Paulo-Brazil, and this soil fulfills the liner bedding characteristics and its gradation toward the finer bond enveloped of underliner materials presented from Lupo and Morrison [21]. For the overliner material, Fleming and Rowe [2] emphasized the use of large stone aggregate to minimize the drainage collection system clogging. Therefore, in this work, it was used a typical Brazilian basaltic drainage aggregate 20/50 mm with D10 25 mm, D30 29 mm, D60 38 mm, a uniformity coefficient of 1.5, and coefficient of gradation of 0.9 for the overliner (Fig. 1b), which was classified as coarse angular poorly graded crushed igneous rock.

Geosynthetics

One of the most common geomembrane materials for liner design in heap leach pads and landfills is High-Density Polyethylene (HDPE) [16, 20]. Also, as reported, an 2.0 or 2.5 mm HDPE thick is required for facilities under high-load conditions [20]. Therefore, the chosen HDPE geomembrane index tensile properties are given in Table 1.

For the propose of this paper, six different protections were examined: protection system A or the no protection, which is the contact of the overliner directly on the geomembrane. Protection system B consists of a single PP nonwoven geotextile layer GT1 mass per unit (MPU) 550 g/m^2 and GT2 MPU 650 g/m^2. Protection system C is a double layer of the GT1 and GT2 denominated, respectively, GT3 and GT4. And at last, protection system D is a 100-mmthick underliner soil placed and compacted above the geomembrane. The PP nonwoven geotextile was chose based on the report by Koerner and Koerner [27]. Table 2 summarizes the main properties of the geotextiles.

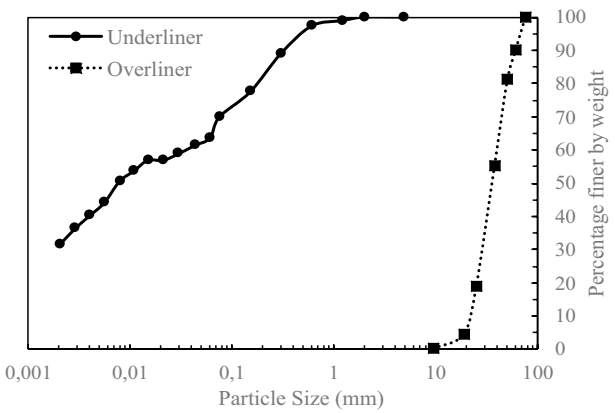

Fig. 2 Grain size distribution of underliner and overliner

Table 1 Geomembrane characteristics

Property	Unit	Value
Polymer	High-density polyethylene	
Density	g/cm^3	0.945 (±0.001)
Thickness	mm	2.08 (±0.036)
Yield strength	kN/m	40.14 (±4.15)
Elongation at yield	%	15.78 (±0.711)
Break strength	kN/m	61.62 (±5.065)
Elongation at break	%	787 (±59.57)
Index puncture	N	804.2 (±63.89)
SCR	hours	1150 (±450)
Tear resistance	N	321.50 (±9.51)
Std. OIT	min	113.25 (±12.73)
CBC	%	2.49 (±0.11)

SCR Stress cracking resistance; *CBC* carbon black content; *Std. OIT* oxidative induction time

Test Apparatus and Procedure

This experiment was carried out by a test apparatus that simulated a liner system, which was used to evaluate the efficiency of protection layers for geomembranes by testing different liner configurations. The apparatus consists of a quadratic box with an inside dimension of 500 × 500 mm and a height of 500 mm. A still plate was placed at the top of the overliner to distribute the applied vertical pressure. No horizontal pressures and lateral strain were considered due to the very stiff steel cell. The friction along the box walls was minimized using two 0.1 mm polyethylene (PE) sheets with grease between them, the first one was attached to the inside wall of the test apparatus and the other was able to move. This configuration reduces boundary friction, and it was also reported by Brachman and Gudina [6] and Dickson and Brachman [24]. All tested sections simulate a single composite liner, which consists of a geomembrane placed over a compacted soil, and its cross-section is illustrated in Fig. 3.

To simulate a firm foundation layer, a 250-mm-thick MH soil was compacted in five 50-mm-thick layers at standard Proctor optimum water contentment of 26–28% and dry density varying from 1490 to 1550 kg/m^3. The

Table 2 Geotextile characteristics

Property	Unit	GT1 Value	GT 2 Value	GT3 Value	GT4 Value
Polymer	Polypropylene (PP)				
Manufacture	Nonwoven, needle-punched, continuous filament				
MPU	g/m^2	550	650	1100	1300
Thickness	mm	3.13	5.43	6.35	11.00

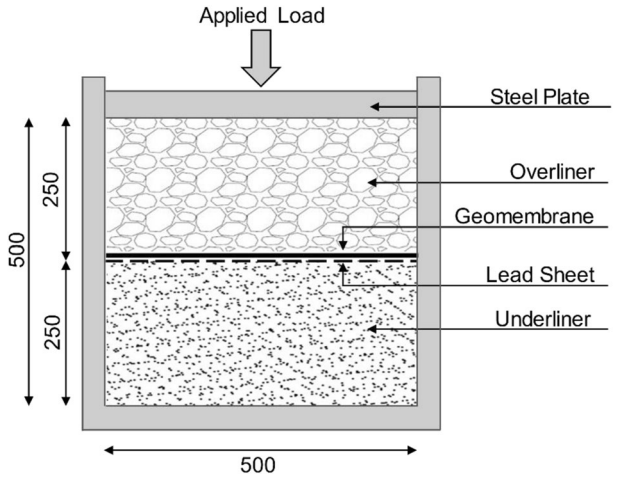

Fig. 3 Test setup (units in mm)

Table 3 Foundation soil geotechnical properties

Property	Unit	Value
USCS classification	MH	
Specific gravity	2.841	
Plastic limit	%	35
Liquid limit	%	59
Max. dry density	kg/m^3	1520
Optimum water content	%	27.0
% Sand	%	10
% Silt	%	60
% Clay	%	30

protection system D had the same compacted conditions than the firm foundation layer, and both were compacted manually by a quadratic hammer of 120 mm and a weight of 40 N dropped from a height of 450 mm. Table 3 summarizes the characterization of the foundation soil. Rowe et al. [26] reported that the underliner gradation, the underliner modulus, and the presence of gravel on the underliner influence the GMB deformations. Therefore, all tests were carefully controlled to present the same soil compaction, and there was no presence of any gravel on the underliner.

A 0.5-mm-thick soft lead sheet (495 × 495 mm) was placed between the underliner and the GMB to record the GMB deformations. After each test, this lead sheet was removed, and the GMB strains were calculated from it. This methodology is the same one reported by Tognon et al. [8] and Brachman and Gudina [18]. Above the GMB it was installed the protection layer and then the aggregate from the overliner was slightly deployed without compaction to prevent the stone locking and the load arching inside the testing box. The aggregate used is in its natural behavior; therefore, any resin was used to mold it. At last, a steel plate was placed upward of the overliner to uniform the applied load.

After the start of each test, the vertical pressure was applied in increments of 360 kPa every 1 h until reaching 1800 kPa pressure for the high-pressure tests or 100 kPa/hour increments until 600 kPa for the low-pressure tests. After that, the pressure was maintained constant for 100 h at 24 ± 2 °C. Sabir and Brachman [22] demonstrated that the geomembrane tensile strains depend on test time, and higher strain values are observed with longer test durations. Therefore, the 100 h test duration represents the less significant differences in strain values over time. The vertical pressure of 1800 kPa admitted at the experiments corresponds to approximately 100 m height heap leach pads since Thiel and Smith [19] reported that the unit weights of crushed ore in heap leach pads are between 1500 and 1800 kg/m^3. On the other hand, the applied pressure of 600 kPa corresponds to a landfill height of 40–60 m when considering the unit weight of 1000 to 1500 kg/m^3 as reported by De Abreu and Vilar [28].

It is essential to highlight the severe conditions this study intends to evaluate with high applied pressure values, the use of coarse gravel and the very soft underline differs from the materials reported by Brachman et al. [25] and Rowe et al. [26]. Therefore, in comparison with other studies, higher strain values are expected. Upon completion of the test, the GMB was visually inspected and quantified the number of punctures, indentations, and grooves. Then, it was classified as "severe" if there is at least one puncture or more than 30 indentations, "moderate" when there is no puncture and were observed > 20 indentations, and "minor" if, in the whole GMB area, there are less than 10 indentations.

Strain Evaluation

At the end of each test, the lead sheet placed between the underlayer and the GMB was removed, and its deformations were scanned by a coordinate measuring machine considering the entire deformed shape of the GMB. The coordinate measuring machine is a device that automatically measures the physical coordinates (X, Y, Z) of an object at different positions on the surface with an optical probe. The three coordinate measurements have a resolution of 1 micron. The outer 45 mm from each side of the 495 × 495 mm lead sheet was not considered to minimize any influences from the edges. Thereby, the scanning surface was a reference to a 450 × 450 mm area.

The GMB strain is calculated along the indentation by dividing the deformed length into segments and assuming that every segment point displaces in the vertical direction. The strain area distribution (SAD) curves were calculated using the methodology developed by Hornsey and Wishow

[11]. It consists of a scanned area with a 1 × 1 mm grid totalizing 160,000 points for each test. For each point, a specific routine was developed to analyze the strain between the eight adjacent points for every location (except edges)–two orthogonal and two diagonal–according to Eq. 1, and it was adopted the highest strain value between them–which consists of the maximum membrane strain outcome. This process was repeated until all strains were calculated across the deformed surface.

$$\varepsilon(\%) = \left[\frac{\sqrt{L^2 + \Delta z^2}}{L} - 1\right].100, \quad (1)$$

where ε is the percentage strain, L the length, and Δz the difference between the original and post-testing height.

It should be noted that the method developed by [11] from Eq. 1 does not correctly calculate the GMB deformed shape as it considers only the vertical displacement of the indentation. [12, 13] presented a method to calculate the maximum GMB strain from irregularly shaped indentations considering the displacement in three directions. Despite the accuracy of the calculating method, the number of segments and the precision of the measurement are significant for the method accuracy. Therefore, considering that any estimated values were obtained by an interpolation processing and the coordinate measuring machine had reading intervals of 1 mm with high precision, the Hornsey and Wishaw's method was appropriated to evaluate the performance of different protection systems under severe conditions.

Results and Discussion

Twelve tests were conducted, and they had the same underliner, overliner, and geomembrane. The differences are at the applied pressure (1800 kPa and 600 kPa) and the protection layers (protection systems A, B, C, or D). For all tests, it was considered that the lead sheet placed beneath the geomembrane represents the geomembrane strains, and the location of these strains is the same for both.

Off the twelve tests realized, no repeatability was analyzed, and it was adopted that the deformed surface of the lead sheet provides good precision. This conclusion was based on the studies by Hornsey and Wishaw [11], which tested five samples of the same configuration, and a good correlation between tests was observed with a coefficient of variation of 0.23%, and Marcotte and Fleming [23] indicated a test precision of approximately 2.7%. Brachman and Gudina [18] indicated that the differences between tests are due to the random distribution and orientation of the contact points between gravel and the geomembrane surface and different geometries of contacts shown to result in different geomembrane strains. Therefore, to control the test precision by using the natural aggregate of this study, it was adopted that the tests with a nonuniform deformed surface of the geomembrane were rejected and repeated.

Table 4 summarizes the adopted configurations, visual inspection status, number of indentations, and percentage of area greater than a proposed limit from all tests evaluated. For evaluating the test results, the calculated GMB strains were analyzed considering both 3% and 6% allowable maximum strain for long-term performance, as recommended by Seeger and Muller [14] and Peggs et al. [15]. However, it can be observed that all the GMB tested in this study have some percentages of the deformed surface exceeding

Table 4 Test conditions and summary of results

Protection system		Applied pressure (kPa)	Visual inspection	Number of indentations	% Area greater than 3% strain	% Area greater than 6% strain
A	No protection	1800	Severe	> 30	61.38	32.02
		600	Moderate	20	40.96	10.80
B	GT1	1800	Severe	> 30	52.53	25.52
		600	Moderate	11	29.75	4.84
	GT2	1800	Severe	> 30	51.13	24.71
		600	Moderate	11	31.45	5.63
C	GT3	1800	Severe	> 30	48.08	18.40
		600	Minor	8	14.48	2.02
	GT4	1800	Severe	> 30	39.76	15.16
		600	Minor	6	12.46	1.46
D	Soil protection	1800	Minor	0	0.12	0.0
		600	Minor	0	0.0	0.0

these proposed limits, and these percentages depend on the applied stress and protection system. Also, it is noteworthy that it is not the focus of this study to suggest what percentage of strain above the threshold is considered acceptable.

Protection System A (No Protection)

The no protection tests were the worst scenario possible. Although in the field some protection above the geomembrane should be used, these tests provide a baseline for comparison with other tests where a protection layer is used. In 1800 kPa pressure, there were two pin-hole punctures (Fig. 4a), the maximum indentation depth at the location of these two punctures was 9.5 mm deep with a maximum strain of 52.88%. Also, there was two other puncture locations that a ductile tear was present and several high strain indentations were observed reaching 61.38% of the area with strain values greater than 3%, which could turn into puncture for long-term performance and lead to more than 650 defects per hectare.

The SAD represented by a deformed surface and a contour map of the no protection tests are given in Fig. 4b for the 1800 kPa pressure and Fig. 4c for the 600 kPa pressure, respectively. There were no punctures for the protection system A, and at 600 kPa pressure, the indentations were less severe, and the area greater than 6% is lower than the 1800 kPa test. However, this test presented a large area exceeding the allowed strain values.

It is evident that when the GMB is in direct contact with gravel, high tensile strains should be expected, and the no protection configuration was too aggressive for the GMB, producing short-term puncture and excessive strains in most of its deformed surface.

Effect of Vertical Pressure on Strain Values for Protection Systems B, C, and D

Protection system B examined the effect of a single layer of a nonwoven geotextile above the geomembrane to reduce the strains and the probability of puncture. For tests using GT1 and GT2 at 600 kPa, the visual inspection verified no puncture in the GMB and a reduction in the number of indentations. An angular aggregate from the overliner caused the indentations that combined with the highest peak strain. However, both tests were still classified as moderately damaged compared to the no protection system.

When comparing the contour maps (Fig. 5a and c) and the percentage of strain above the proposed limits from Table 4, both single-layer nonwoven geotextile protection (protection system B) had similar values. However, despite the geotextiles preventing puncture and reducing the area percentage above the strain limit, there were still significant indentations and strains, which, according to [17], could lead to long-term tensile stress due to stress crack.

In the second case, increasing the pressure to 1800 kPa (Fig. 5b and d), the single protection barely reduces the strains when compared with the no protection test, resulting in maximum strain values above 45% and with indentations depth above 9 mm for both GT1 and GT2. Also, the visual inspection reveals several indentations and pin-hole punctures. Thus, the protection system B was insufficient to prevent significant strains and punctures and hence unsuitable for these severe conditions.

Protection system C consists of a double nonwoven geotextile above the GMB. For the applied pressure of 600 kPa (Fig. 6a and c), there were eight and six indentations with strain exceeding the adopted threshold for tests with GT3 and GT4, respectively. The visual inspection showed that protection system C increased the protection efficiency from moderate (protection systems A and B) to minor. The maximum strain of 11% calculated at the side of a 5.5 mm indentation for the GT3 exceeds the 8.5% and 4.5 mm indentation obtained from GT4, suggesting that the role of the geotextile protection can be dependent on factors other than MPU. Thus, while there is some variability from GT3 and GT4, the percentage of the area above the proposed limit for the GMB deformed surface was less severe than protection systems A and B.

Despite the double nonwoven geotextile protection above the GMB (protection system C), when increasing the vertical pressure to 1800 kPa, both GT3 (Fig. 6b) and GT4 (Fig. 6d) protection geotextiles were not able to prevent puncture of the GMB as three pin-hole punctures, and several indentations points were observed in the visual analyses. When comparing the contour maps, the area with strain above the limit was smaller than the protection systems A and B. However, the maximum strain of 43.43% and 31.22% for GT3 and GT4 are still high strain values.

The severe conditions of the experiment can justify the high strain values obtained with the protection systems A, B, and C. In other words, the underliner utilized has a high plasticity index, which according to Marcotte and Fleming [23] increases the magnitude of the GMB strains. Also, Brachman and Gudina [18] demonstrated that the nominal grain size of the gravel influenced the maximum tensile strain, and the aggregate with a 50 mm nominal grain size was the worst condition tested.

Efficiency of Different Protection Layers

The amount of strain in the geomembrane can be represented by the percentage of the overall geomembrane area in which the allowable maximum threshold strain is exceeded [11, 23].The cumulative distribution graph allows visualization and comparison between the strains at any level to the total

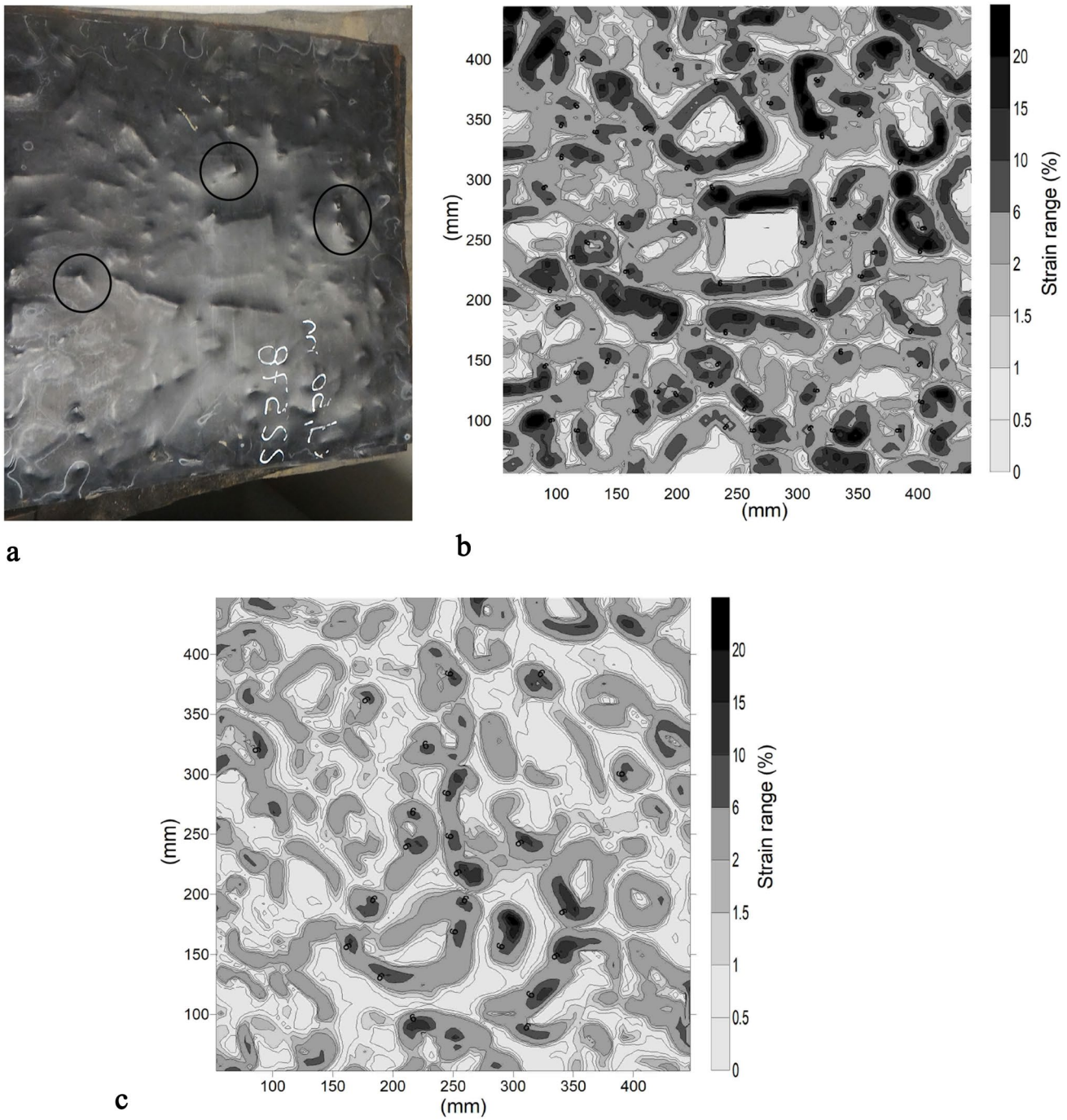

Fig. 4 **a** Photograph of the geomembrane from test no protection 1800 kPa. **b** Deformed surface for no protection 1800 kPa. **c** Deformed surface for no protection 600 kPa

area in different protection layers of the geomembrane tested (Fig. 7).

Comparing the percentage of strain values from both tests (600 and 1800 kPa), the presence of single geotextile protection (GT1 and GT2) was not able to significantly reduce the percentage area of strain below the 3% threshold in comparison with the no protection test. However, protection system B significantly reduced the high strain values (above 6%), especially for the 600 kPa configuration.

By increasing the MPU of the geotextile protection layer, it is evident that lower strain values are presented. However, GT2 has a higher MPU area and thickness than GT1, and for the single geotextile protection, both had similar efficiency (Fig. 7a and b). On the other hand, for

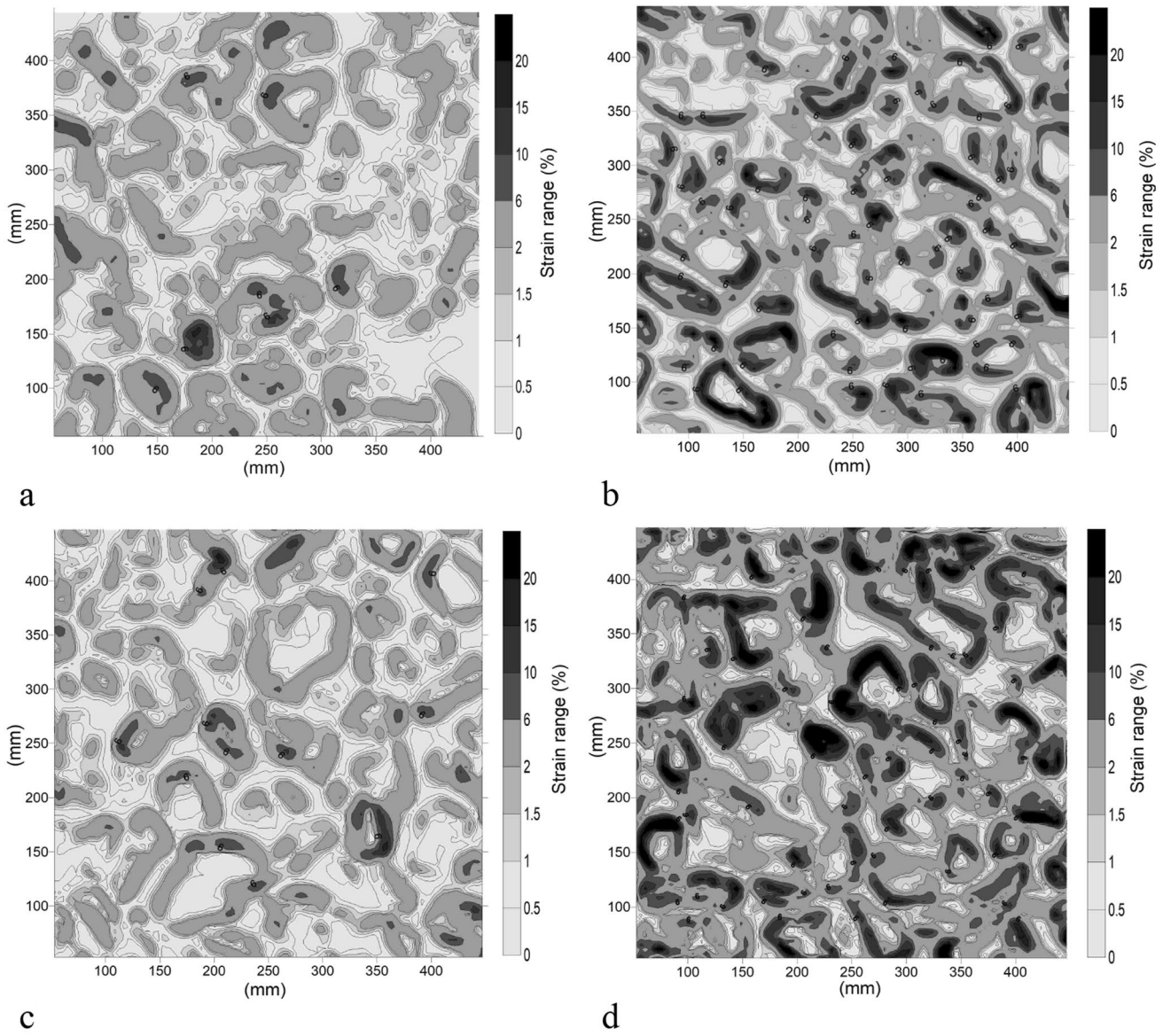

Fig. 5 Deformed surface of the GMB for **a** GT1 (600 kPa). **b** GT1 (1800 kPa). **c** GT2 (600 kPa). **d** GT2 (1800 kPa)

double geotextile protection, GT4 showed better performance than GT3. These results showed the limitation of using only unit weight to specify a protection geotextile; similar considerations were noted in Rowe and Yu [16].

The protection system D tests consist of placing and compacting a 100 mm underline soil above the geomembrane, protecting it from puncture. These configurations proved to be the most effective protection systems, limiting the maximum strain to 1.5% and the maximum indentation to 1.5 mm. When analyzing the whole deformed surface, almost 100% of the strain values were concentrated in the 0–0.25% range, as presented in Table 4. Thus, in this case, the maximum strain values reported probably occur by the differential settlements of the underliner and not from the granular material from the overliner.

Compared with other studies, Gudina and Brachman [6] and Brachman and Gudina [18] also showed that a single nonwoven geotextile was insufficient to limit tensile strains to allowable levels from a nominal 50 mm coarse gravel. In different test configurations, Dickson and Brachman [24] and Brachman et al. [25] also demonstrated that soil protection limited the geomembrane tensile strain to values below 1%. Although soil protection proved the most efficient protection layer, it cannot be considered part of the drainage layer [1]. Furthermore, the work of Giroud [29] indicates that damage in the GMB during construction often is caused by the

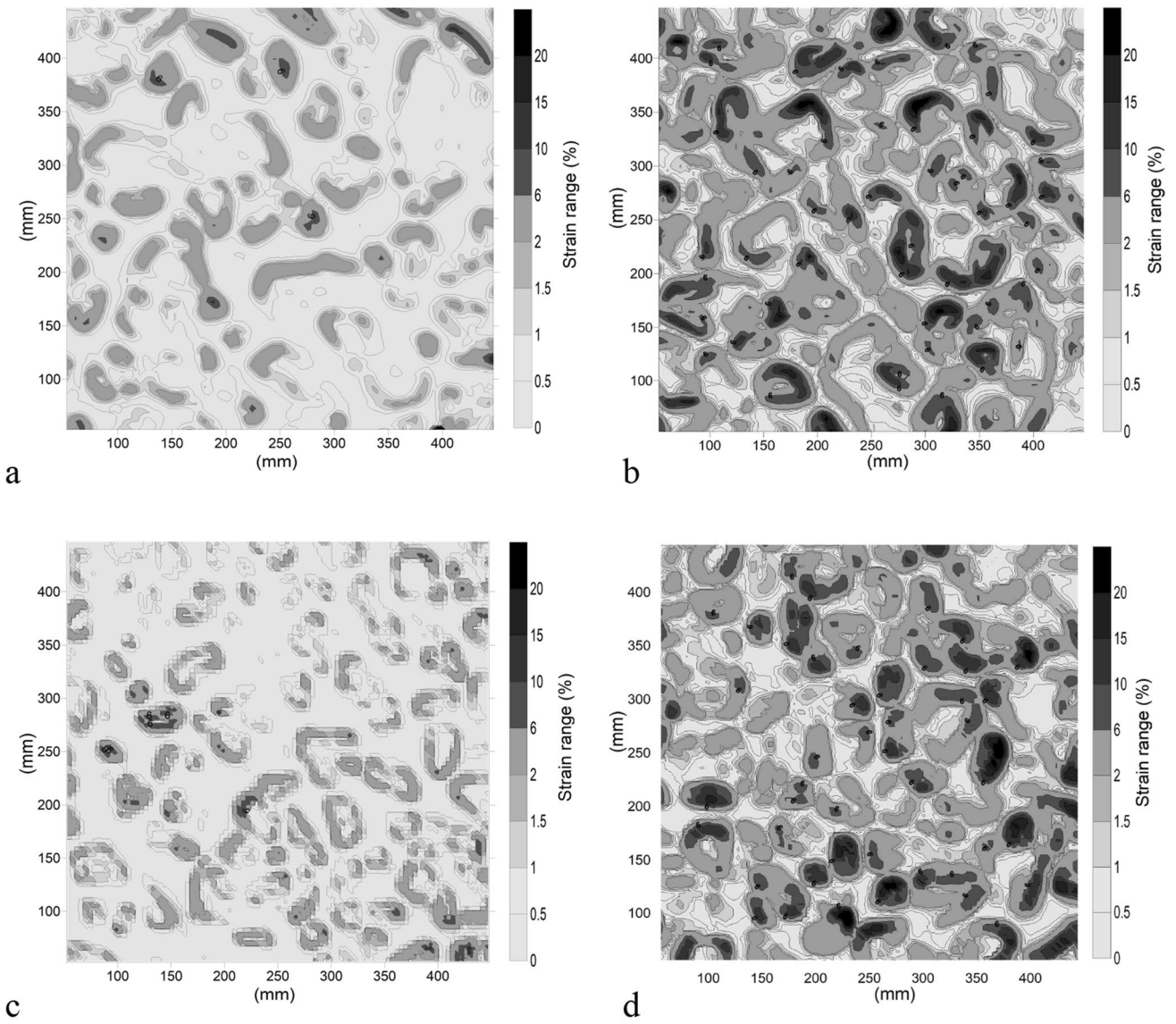

Fig. 6 Deformed surface of the GMB for **a** GT3 (600 kPa); **b** GT3 (1800 kPa); **c** GT4 (600 kPa); **d** GT4 (1800 kPa)

placement of soil layers on top of it. Another limitation of using soil as a protection layer is that it can function as a diffusion barrier lowering the hydraulic conductivity and increasing the leachate head above the geomembrane [1].

Conclusions

A quadratic box with an inside dimension of 500 × 500 mm and height of 500 mm was used to simulate a single composite liner system, composed of a 2.0 mm GMB placed over a compacted clayed soil. The focus of this paper was to evaluate the influence of a single nonwoven geotextile (GT1 and GT2), double nonwoven geotextile (GT3 and GT4), and a soil protection on development of tensile strain in the GMB from a 50 mm coarse gravel subjected to a 600 kPa and 1800 kPa pressure. The results were analyzed using a strain map of the distribution of localized tensile strain in the geomembrane and were evaluated from the threshold value for maximum allowable strain of 3% and 6%. The following conclusions presented in this paper reflect only the test conditions examined:

- For the GMBs tested at 1800 kPa, the protection system A presented 2 punctures and 60% of the area with high strain values for the high applied stress. The protection systems B and C were unable to prevent puncture of the GMB and reduced only 10% of the strain area above 3%. Although protection system C (double nonwoven geotextile) reduced the strain values, the GMB area exhibiting

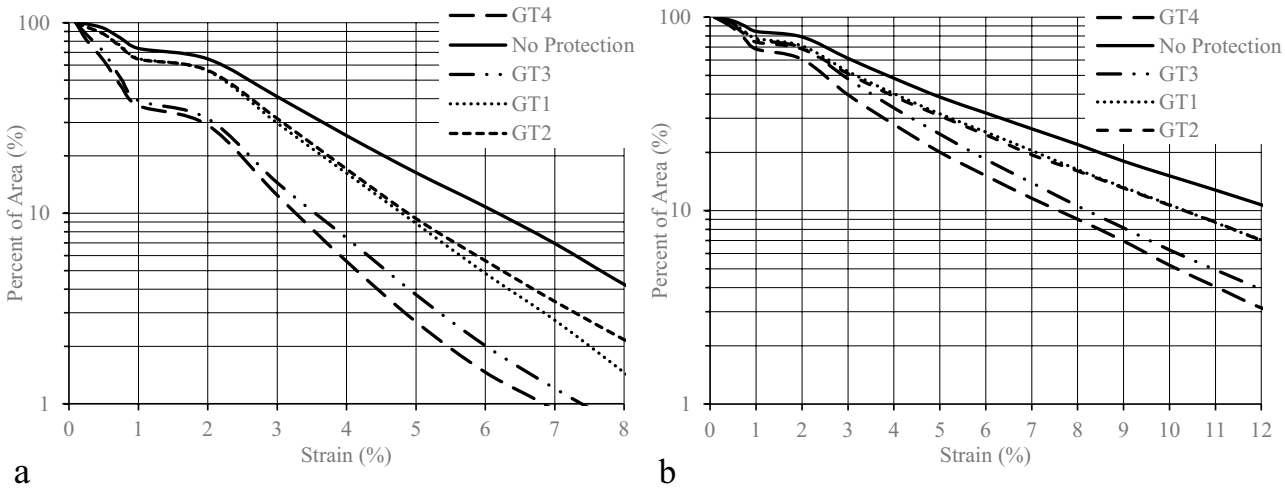

Fig. 7 Strain evaluation for **a** 600 kPa. **b** 1800 kPa

strain above the 3% limit was too high (48% GT3 and 39% GT4) and could lead to long-term failure.

- For the GMBs tested at 600 kPa applied pressure, the geotextile protections were able to reduce the GMB strain as GT1, GT2, GT3, and GT4 had approximately 30, 31, 14, and 12%, respectively, of the area exceeding the 3% threshold, which is a reduction of the 41% of the no protection test configuration. However, even considering the most conservative proposed limit, all tests from protection systems A, B, and C showed a percentage of area with strain above the most conservative proposed limit. These results suggest the need for a future study of the required efficiency of what percentage of strain above the threshold is considered acceptable.
- The role of MPU of the geotextile has been shown to exhibit a significant influence on the deformation of the GMB. The double geotextile decreased the GMB area exceeding the threshold strain when compared with no protection system. However, the results suggest a limitation of using only MPU to specify a protection geotextile, as GT4 (thicker geotextile) had better performance in reducing the geomembrane strain with reductions of 22% and 29%, in comparison to 13% and 27% reduction for GT3 with a similar MPU.
- Of all the different protection layers tested, only the 100 mm soil protection layer was able to reduce the whole deformed surface of the geomembrane to strain values lower than 2% for both the applied pressures. Although soil protection proved the most efficient protection layer, it cannot be considered part of the drainage layer, as it used the same clayed soil of the underliner in the tests. Also, considerations of the potential damage from the construction equipment, difficulties with trafficability during rain, the presence of gravel in the soil, and the high costs for construction must be taken into account.

Acknowledgements The authors are indebted to the following institutions that supported the research activities reported in this paper in different ways: National Council for Scientific and Technological Development (CNPq) and University of São Paulo (USP), and CAPES–Brazilian Ministry of Education. The authors also thank the manufacturer of geosynthetics TDM Brazil and Mexichem Brazil–Bidim for providing information and materials presented in this paper.

Author Contributions All the authors listed have made a substantial, direct and intellectual contribution to the work, and approved it for publication.

Data Availability The datasets generated for this study are available on request to the corresponding author.

Declarations

Conflict of interest On behalf of all the authors, the corresponding author states that there is no conflict of interest.

References

1. Rowe RK (2005) Long-term performance of contaminant barrier systems. Geotechnique 55(9):631–678. https://doi.org/10.1680/geot.2005.55.9.631
2. Fleming IR, Rowe RK (2004) Laboratory studies of clogging of landfill leachate collection and drainage systems. Can Geotech J 41:134–153. https://doi.org/10.1139/t03-070
3. Rowe RK, Fan J (2022) A general solution for leakage through geomembrane defects overlain by saturated tailings and underlain by highly permeable subgrade. Geotext Geomembr 50:694–707. https://doi.org/10.1016/j.geotexmem.2022.03.010
4. Marcotte BA, Fleming IR (2020) Damage to geomembrane liners from tire derived aggregate. Geotext Geomembr 48:198–209. https://doi.org/10.1016/j.geotexmem.2019.11.005

5. Narejo DB, Koerner RM, Wilson-Fahmy RF (1996) Puncture protection of geomembranes Part II: experimental. Geosynth Int 3(5):629–653. https://doi.org/10.1680/gein.3.0078
6. Gudina S, Brachman RWI (2006) Physical response of geomembrane wrinkles overlying compacted clay. J Geotech Geoenviron Eng 132(10):1346–1353. https://doi.org/10.1061/ASCE1090-02412006132:101346
7. Dickinson S, Brachman RWI (2006) Deformations of a geosynthetic clay liner beneath a geomembrane wrinkle and coarse gravel. Geotext Geomembr 24:285–298. https://doi.org/10.1016/j.geotexmem.2006.03.006
8. Tognon AR, Rowe RK, Moore ID (2000) Geomembrane strain observed in large-scale testing of protection layers. J Geotech Geoenviron Eng 126(12):1194–1208. https://doi.org/10.1061/(ASCE)1090-0241(2000)126:12(1194)
9. Abdelaal FB, Rowe RK, Brachman RWI (2014) Brittle rupture of an aged HPDE geomembrane at local gravel indentations under simulated field conditions. Geosynth Int 21:1–23. https://doi.org/10.1680/gein.13.00031
10. Brachman RWI, Asce M, Sabir A (2013) Long-term assessment of a layered-geotextile protection layer for geomembranes. J Geotech Geoenviron Eng 139(5):752–764. https://doi.org/10.1061/(ASCE)GT.1943
11. Hornsey WP, Wishaw DM (2012) Development of a methodology for the evaluation of geomembrane strain and relative performance of cushion geotextiles. Geotext Geomembranes 35:87–99. https://doi.org/10.1016/j.geotexmem.2012.05.002
12. Eldesouky HMG, Brachman RWI (2018) Calculating local geomembrane strains from a single gravel particle with thin plate theory. Geotext Geomembr 46:101–110. https://doi.org/10.1016/j.geotexmem.2017.10.007
13. Eldesouky HMG, Brachman RWI (2023) Calculating local geomembrane strains from gravel particle indentations with thin plate theory. Geotext Geomembr 51:56–72. https://doi.org/10.1016/j.geotexmem.2022.09.007
14. Seeger S, Muller W (1996) Requirements and testing of protective layer systems for geomembranes. Geotext Geomembr 14:365–376. https://doi.org/10.1016/0266-1144(96)89792-5
15. Peggs ID, Schmucker B, Carey P (2005) Assessment of maximum allowable strains in polyethylene and polypropylene geomembranes. In: Proc, Geo- frontiers 2005, Austin, Texas. https://doi.org/10.1061/40789(168)23
16. Rowe RK, Yu Y (2019) Magnitude and significance of tensile strains in geomembrane landfill liners. Geotext Geomembr 47:439–458. https://doi.org/10.1016/j.geotexmem.2019.01.001
17. Zanzinger H (1999) Efficiency of geosynthetic protection layers for geomembrane liners: performance in a large-scale model test. Geosynth Int 6(4):303–317. https://doi.org/10.1680/gein.6.0155
18. Brachman RWI, Gudina S (2008) Gravel contacts and geomembrane strains for a GM/CCL composite liner. Geotext Geomembr 26:448–459. https://doi.org/10.1016/j.geotexmem.2008.06.001
19. Thiel R, Smith ME (2004) State of the practice review of heap leach pad design issues. Geotext Geomembr 22:555–568. https://doi.org/10.1016/j.geotexmem.2004.05.002
20. Lupo JF (2010) Liner system design for heap leach pads. Geotext Geomembr 28:163–173. https://doi.org/10.1016/j.geotexmem.2009.10.006
21. Lupo JF, Morrison KF (2007) Geosynthetic design and construction approaches in the mining industry. Geotext Geomembr 25:96–108. https://doi.org/10.1016/j.geotexmem.2006.07.003
22. Sabir A, Brachman RWI (2012) Time and temperature effects on geomembrane strain from a gravel particle subjected to sustained vertical force. Can Geotech J 49:249–263. https://doi.org/10.1139/T11-096
23. Marcotte BA, Fleming IR (2019) The role of undrained clay soil subgrade properties in controlling deformations in geomembranes. Geotext Geomembr 47:327–335. https://doi.org/10.1016/j.geotexmem.2019.02.001
24. Dickinson S, Brachman RWI (2008) Assessment of alternative protection layers for a geomembrane - geosynthetic clay liner (GM-GCL) composite liner. Can Geotech J 45:1594–1610. https://doi.org/10.1139/T08-081
25. Brachman RWI, Rowe RK, Irfan H (2014) Short-term local tensile strains in HDPE heap leach geomembranes from coarse overliner materials. J Geotech Geoenviron Eng 140(5):04014011. https://doi.org/10.1061/(asce)gt.1943-5606.0001087
26. Rowe RK, Brachman RWI, Irfan H et al (2013) Effect of underliner on geomembrane strains in heap leach applications. Geotext Geomembr 40:37–47. https://doi.org/10.1016/j.geotexmem.2013.07.009
27. Koerner GR, Koerner RM (2011) Puncture resistance of polyester (PET) and polypropylene (PP) needle-punched nonwoven geotextiles. Geotext Geomembr 29:360–362. https://doi.org/10.1016/j.geotexmem.2010.10.008
28. De Abreu AES, Vilar OM (2016) Accessing the biological stability of municipal solid waste of different landfilling ages. J Solid Waste Technol Mngmnt 42:236–244. https://doi.org/10.5276/JSWTM.2016.236
29. Giroud JP (2016) Leakage control using geomembrane liners. S&R 39(3):213–253. https://doi.org/10.28927/SR.393213